

A Unified Integrated PHEV with Interleaved Boost Converter for Power Factor Correction Applications using SRM

G.VAMSI KRISHNA, ASSISTANT PROFESSOR, kvamsi706@gmail.com

P.SANJANNA, ASSISTANT PROFESSOR, sanjana@svitap.ac.in

B.ARUNA, ASSISTANT PROFESSOR, bonasiaruna@gmail.com

Department of Electrical & Electronics Engineering, Sri Venkateswara Institute of Technology, N.H 44, Hampapuram, Rapthadu, Anantapuramu, Andhra Pradesh 515722D

Abstract:

Because of their increasing popularity, this article focuses on plug-in hybrid electric vehicles (PHEVs), which are known for their extended range, excellent fuel efficiency, and low carbon emissions. With fewer power electronic components required than traditional topologies, this study introduces an optimised switching reluctance motor (SRM) powertrain architecture for plug-in hybrid electric vehicles (PHEVs). Depending on the road conditions, you may choose from four different driving modes in motor driving mode. Driving and braking activities may be integrated efficiently. Without the need for external

Keywords:

Battery, Interleaved Boost Converter, PHEVs, PFC, SRM, and other related

battery chargers, three charging ways are capable of charging the battery. A three-channel interleaved boostconverter with power factor correction (PFC) capabilities is constructed using the SRM windings and integrated converter circuit to charge the traction battery from the grid. A built-in half-bridge isolation dc/dc converter is used to transfer power from the generator or traction battery to the auxiliary battery. The suggested integrated drive architecture and associated control techniques are simulated on a three-phase 12/8 poles SRM to ensure their practicality.

terms.

1. Introduction

A combination of environmental concerns and economic pressures has led to the rise in popularity of electric cars (EVs), hybrid electric vehicles (HEVs), and plug-in hybrid electric vehicles (PHEVs), all of which reduce pollutants and improve fuel efficiency. From [1] to [3]. The advantages of both conventional HEVs and electric cars are combined in a plug-in hybrid, or PHEV. It outperforms HEVs in terms of fuel efficiency and has a greater range than EVs. The only way for a hybrid electric vehicle's battery bank to be charged is via the

generator that is powered by the ICE. Charging the PHEV's battery bank is possible via the grid, however. At this stage of battery technology, PHEVs are more acceptable due to their fuelling flexibility [4]-[7].

The electric drive system is a crucial component of plug-in hybrid electric vehicles (PHEVs), and among electric motors, the interior permanent magnet synchronous motor (IPMSM) is often used in HEVs and PHEVs because of its efficiency and high power density. [8]. The

use of rare-earth elements in NdFeB permanent magnets is one of the main concerns with mass-producing HEVs, however this is not the case with an IPMSM [9], [10].

The switching reluctance motor (SRM) is a rare-earth-free motor that is very competitive in transportation applications due to its robust construction, strong starting torque, broad speed range, inherent fault tolerance, and excellent operational efficiency [11]-[13]. When space is at a premium, PHEVs may not be the best option, and increasing the motors' power density won't cut it. Reusing the traction motor and power electronics in an integrated electrical powertrain with battery charging capabilities is an attractive alternative, but the power converter in the electric drive system has to be well-designed. For the integrated onboard charger (OBC) for PHEVs, many motor types have been considered, including induction motors, permanent magnet synchronous motors, and SRM. The traction engines

and traction battery to auxiliary battery (T2A). Capacitors C1 and C2, the rectifier, the SRM winding and its power converter, and many other components all serve many purposes in the suggested converter's several modes of operation. The suggested integrated powertrain differs from the other topologies in that it offers additional operating modes and faster integration speeds. For SRM to work in PHEVs, the electric drive system has to be smaller and cheaper. Strategies for controlling driving and charging modes are also suggested in order to complete the related duties.

The power converter and stator windings are transformed into a boost battery charger, with the addition of an external power rectifier and LC filter.

Using the SRM in a PHEV programme isn't without its challenges, one of which is the unique power converter. The article explains how PHEVs may benefit from an optimised power converter that uses a reduced power unit. Motor operating modes allow the SRM to switch between the traction battery, the generator, or both, allowing it to adapt to different road conditions. You can drive and brake with ease using the proposed topology. For charging the attraction battery in battery charging mode, a three-channel interleaved boost power factor correction (PFC) converter is used, which consists of the rectifier, SRM windings, and power converter. The windings of the SRM may be employed as filter inductors and energy storage for the OBC without any changes. There are three charging modes that may be achieved by using the stator windings and optimised power converter for SRM. These modes include grid to traction battery (G2T), generator to auxiliary battery (G2A),

2. Integrated SRM Powertrain Topology for PHEV

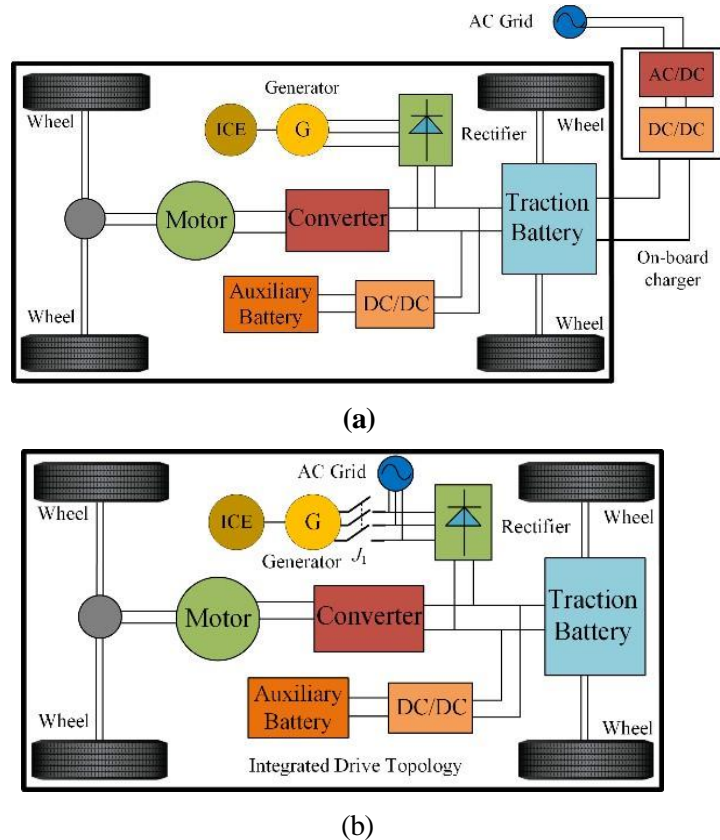


Figure.1 Schematic of the PHEV powertrain. (a) Traditional powertrain. (b) Proposed powertrain.

Figure. 1 illustrates a diagram of the PHEV powertrain. A conventional electrified powertrain, as seen in Figure. 1(a), consists of an ICE, a generator powered by the ICE for converting mechanical energy to electrical energy, a rectifier for rectification, a main energy storage source, i.e., a traction battery bank for propulsion, a traction motor or an independent dc/dc converter for connecting the auxiliary battery to the dc-link bus, a main converter for charging the driving motor, a traction motor also coupled to a mechanical driveline, and an auxiliary battery for automotive electronics. The traction battery is usually charged using an on-board charger (OBC) that has an ac/dc converter, a dc/dc converter, and certain inductors and capacitors. Figure 1(b) shows the suggested integrated drive architecture, which aims to enhance the degree of integration. We have discontinued the standalone OBC. The generator and

motor's current power converters serve as filter inductors, while the motor's windings comprise the ac/dc and dc/dc converters aimed at the OBC. An additional relay J1 is used to connect and detach the generator from the rectifier. The configuration of a three-phase 12/8 poles SRM is shown in Figure 2(a). Phase A is formed by connecting the windings on four poles in sequence. The phase A winding is shown by the LA in Figure 2(a). Like phase A, phases B and C have the same winding connections. In Figure 2(b), we can see a schematic representation of the suggested integrated SRM drive geometry. Due to their mechanical coupling, the internal combustion engine (ICE) and generator work together to provide three-phase alternating current (ac) electricity. After

the generator, a diode-bridge rectifier is used to convert alternating current (ac) to direct current (dc). The battery bank are not running. Before the rectifier is installed, an EMI filter is used to prevent the transmission of electromagnetic interference (EMI)

may be charged from the electrical grid using a grid adaptor when the internal combustion engine and generator noise from the battery side. A relay J1 is connected to disconnect the generator from the grid while the traction battery charging mode is in use.

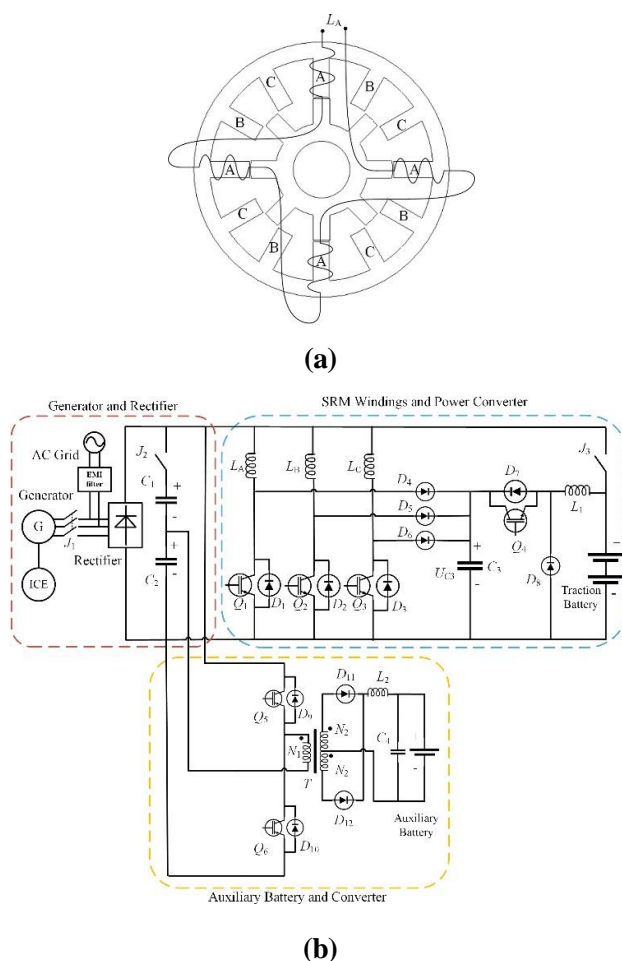


Figure.2Diagram of the SRM drive converter for PHEV. (a) Structure of the SRM. (b) Detailed diagram of the proposed integrated converter.

The Los Angeles, LB, and LC windings provide three phases in an SRM. Q1–Q4 insulated gate bipolar transistors (IGBTs), D1–D8 diodes, L1 inductor, and C3 capacitor make up the SRM power converter. A half-bridge isolation dc/dc converter for charging the auxiliary battery consists of inductor L2, capacitor C4, transformer T, and integrated gate bipolar transistors (IGBTs) Q5 and Q6. It also contains

diodes D9, D10, D11, and D12. The half-bridge isolation dc/dc converter, which charges the auxiliary battery, also includes the dc-link bus capacitors, which are connected in series as C1 and C2. The traction battery powers the propulsion engine, while the auxiliary battery powers the onboard electrical gadgets. The usage of relays J2 and J3 allows for the realisation of a number of operational modes.

PHEV Driving Modes

When the PHEV is in driving mode, the load circumstances determine whether the traction battery or the generator, or both, will power the vehicle. This is accomplished by turning on relay J2. Winding demagnetization, winding excitation, and demagnetization energy recovery are the three modes described above.

- Propelled by a Traction Battery on its own
- Propelled by a Generator on its own
- Propelled by a Traction Battery and Generator Working Together
- Recovering Energy from Demagnetization

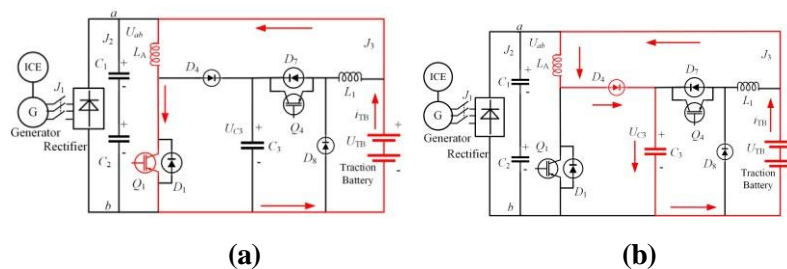


Figure.3 Driven by traction battery-alone. (a) Winding excitation state. (b) Winding demagnetization state.

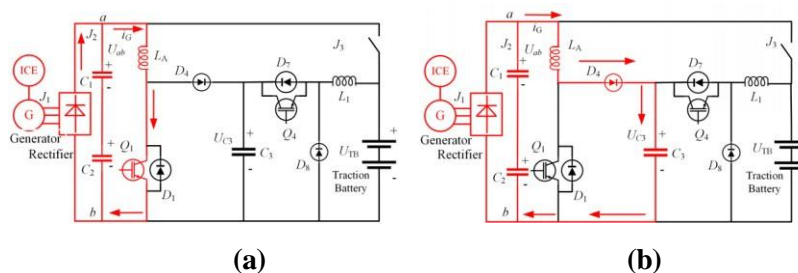


Figure.4 Driven by generator-alone. (a) Winding excitation state. (b) Winding demagnetization state.

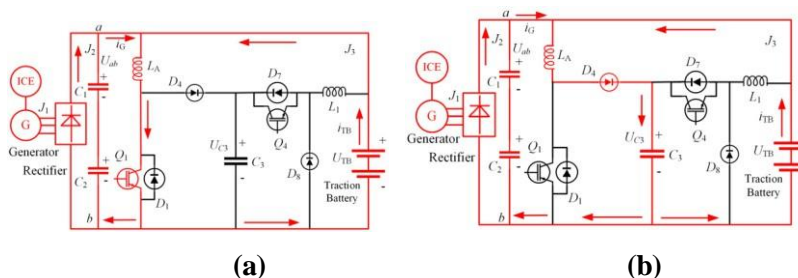


Figure.5 Driven by traction battery and generator together. (a) Winding excitation state. (b) Winding demagnetization state.

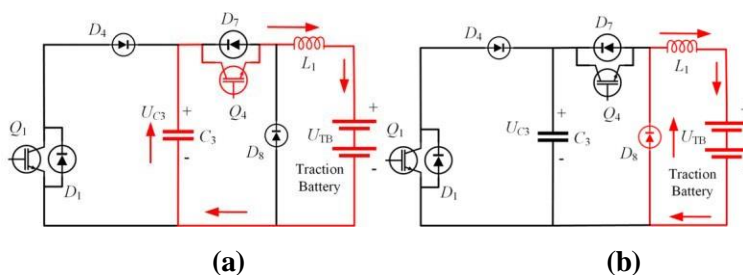


Figure.6 Demagnetization energy recovery. (a) Stage 1. (b) Stage 2.

PHEV Battery-Charging Modes

The planned optimized drive topology requires onboard charging, which reduces the need for a separate battery charger. According to the driver's order, the battery banks may be charged by a generator or the grid. The integrated topology will accommodate three separate battery-charging modes: G2T mode, G2A

mode, and T2A mode.

- Traction Battery Charged by Grid (G2T)
- Auxiliary Battery Charged by Generator (G2A)
- Auxiliary Battery Charged by Traction Battery (T2A)

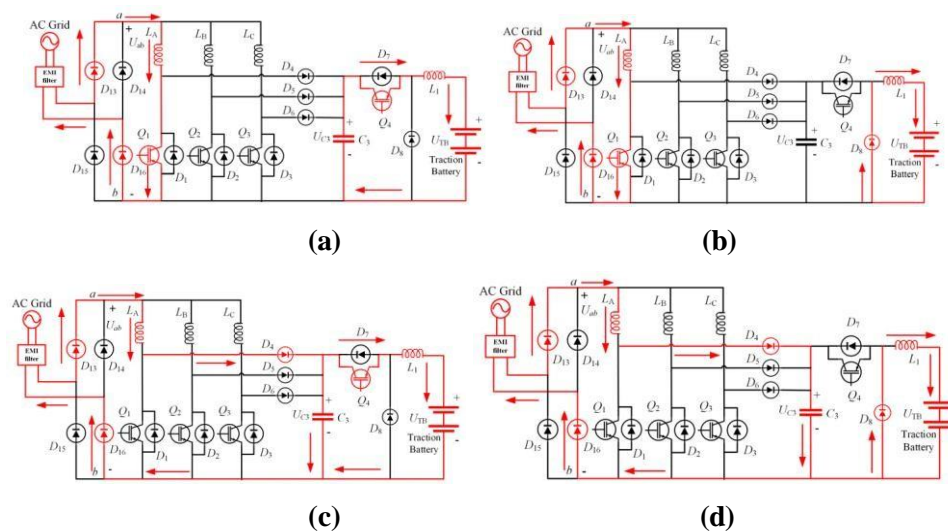


Figure.7 Traction battery charged by the grid. (a) Stage 1. (b) Stage 2. (c) Stage 3. (d) Stage 4.

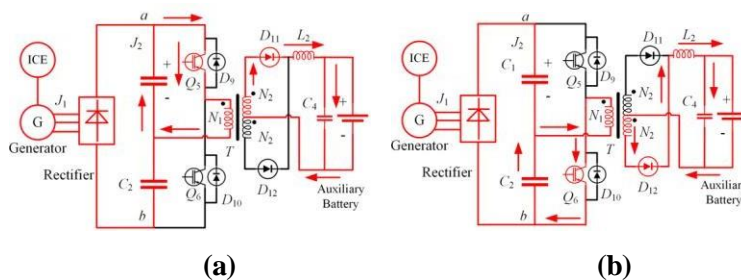


Figure.8 Auxiliary battery charged by the generator. (a) Stage 1. (b) Stage 2.

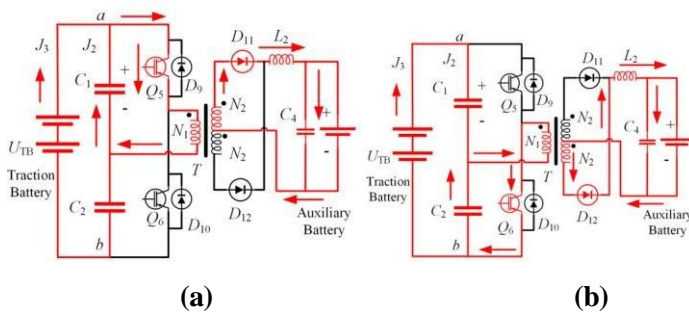


Figure.9 Auxiliary battery charged by traction battery. (a) Stage 1. (b) Stage 2.

3. Control Schemes for Motoring and Charging Modes

PHEV Driving Control Strategy

Figure. 10 shows the control technique in driving mode as a block diagram. For phase current closed-loop operation, the current hysteresis controller is chosen due to its high resilience and easy design. At 13 kHz, the sampling frequency is 2 A, and the current hysteresis bandwidth is 1.2. The input is

the difference in actual current values (i_A , i_B , and i_C) from the required value (i).

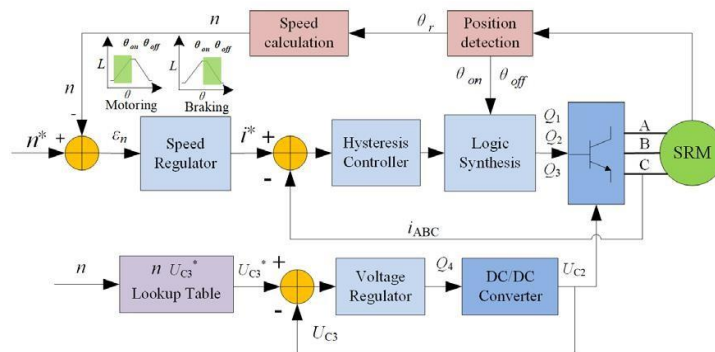


Figure.10Diagram of the driving control strategy.

Q1, Q2, and Q3 are the switching signals generated by the logic synthesis unit by the integration of ON, OFF, and hysteresis signals. Using the PI regulator and the input n = difference between the specified rotor speed n and the actual rotor speed n allows for speed closed-loop control. The output is the supplied current value i^* for the inner current regulator. When the speed is less than the basic speed, which is 1000 r/min, the UC_3 is set to 72 V. The amount of time needed to demagnetize an object throughout one electrical cycle decreases as the rotational speed rises once it reaches the base speed. The UC_3 develops a linear relationship with increasing rotational speed from 1000 to 2000 r/min, ultimately reaching 108 V. A PI regulator is used in the closed-loop control of the voltage UC_3 by modifying the service cycle of switch Q4.

3.2 Strategy for Controlling Battery Charging

The control block diagrams for the G2T mode are shown in Figure 11. Two closed-loops comprise the controller for the interleaved boost converter, as shown in Figure 11 (a). A current inner loop PI regulator is used to regulate the capacitor C3 voltage UC_3 and output the amplitude of the reference value I^* . By multiplying I^* by the cos and absolute value (ABS) modules, we can get the instantaneous current reference value (ref), which is derived from the

grid voltage phase angle sensed by the phase-locked loop (PLL).

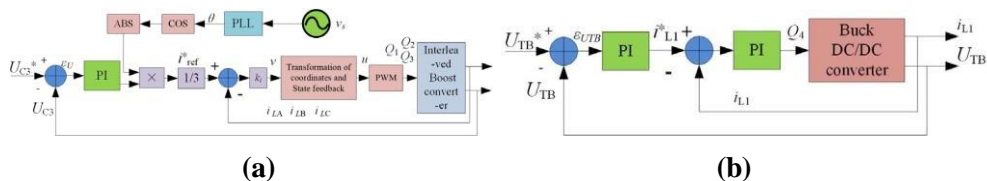


Figure.11Block diagrams of the control system for G2T mode. (a) Interleaved boost converter. (b) Buck converter.

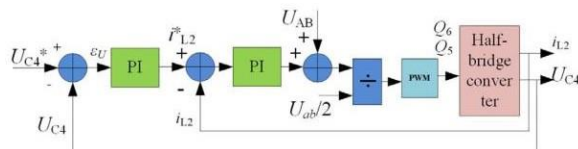


Figure.12.Block diagrams of the control system for G2A and T2A modes.

SRM in order to verify the effectiveness of the proposed integrated SRM drive topology and control strategies. The controller's diagram is seen in Figure. 13.

TABLE I
SRM DRIVE SYSTEM SPECIFICATION

| Specifications | Value |
|-------------------------------|-------|
| Phase number | 3 |
| Stator/rotor poles | 12/8 |
| Rated power (W) | 750 |
| Rated speed (r/min) | 1000 |
| Minimum phase inductance (mH) | 0.3 |
| Maximum phase inductance (mH) | 1.6 |

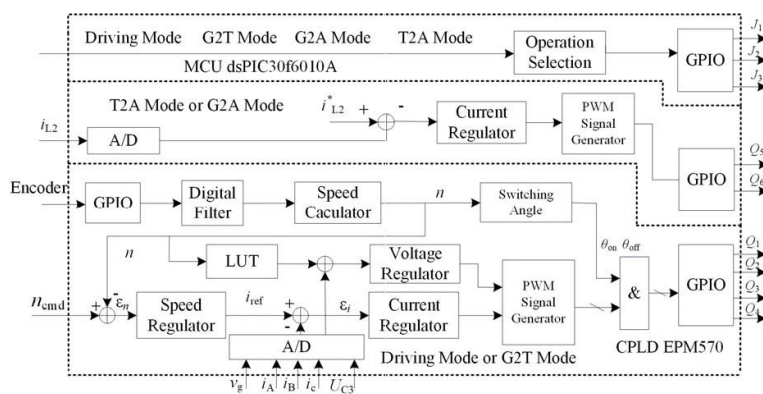


Figure.13.Schematic of the controller.

Figure. 14 displays the waveforms of multiple drive modes at 500r/min, where i_A represents phase A phase current, i_g represents generator output current, i_{TB} represents traction battery

current, and U_{C3} represents capacitor C_3 voltage. The SRM is operated independently by the traction battery in battery driving mode, and the generator is idle, as seen in Figure. 14.

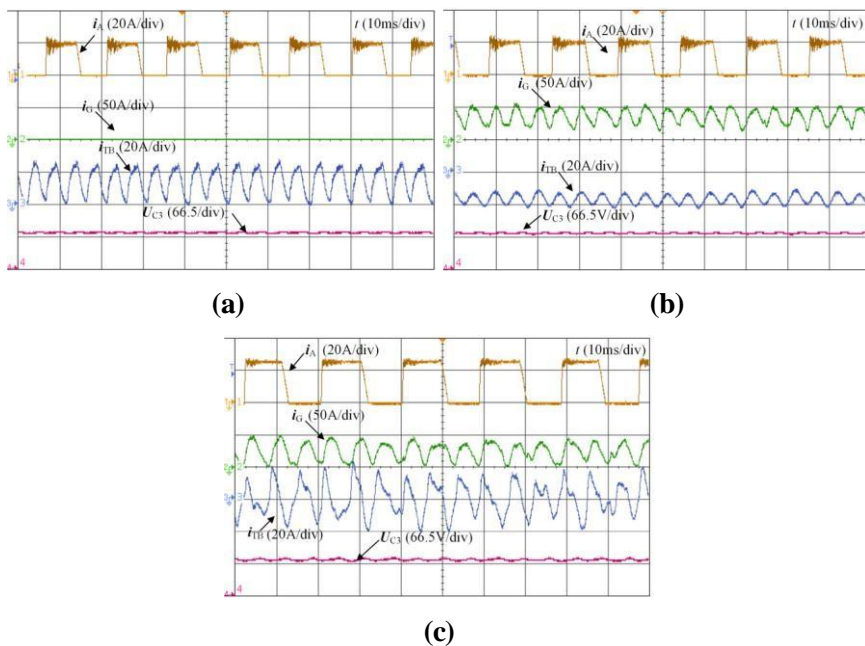


Figure.14Low-speedoperation.(a)Batterydrivingmode.(b)Generatordriving mode. (c) Battery and generator driving mode.

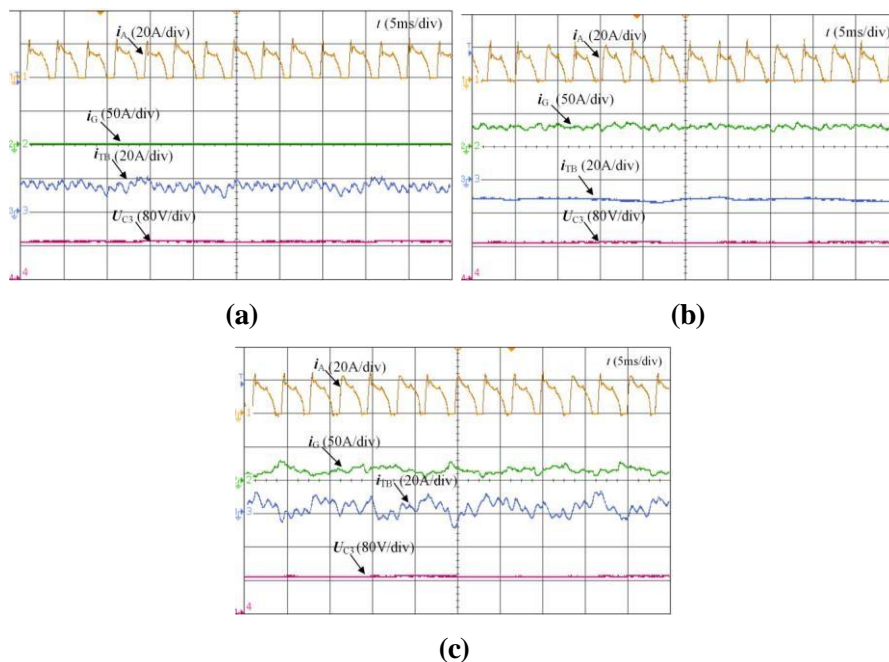


Figure.15High-speedoperation.(a)Batterydrivingmode.(b)Generator driving mode. (c) Battery and generator driving mode.

Shown in Figure 15 are the simulation waveforms taken at a motor speed of about 2000 r/min. While operating at high speeds, the modes are quite similar to those while providing low speeds of service. Output currents from the traction battery, as well as the generator,

are more uniform than they are during low-speed operations.

Figure.16 shows the simulated results of changing the action from driving to braking. In Figures, you can observe the expanded views of Figures 16(a) and (c).

and(d), in that order. CH1 is the brake signal and CH3 is the phase A drive signal in Figure.16(c) and (d), respectively.

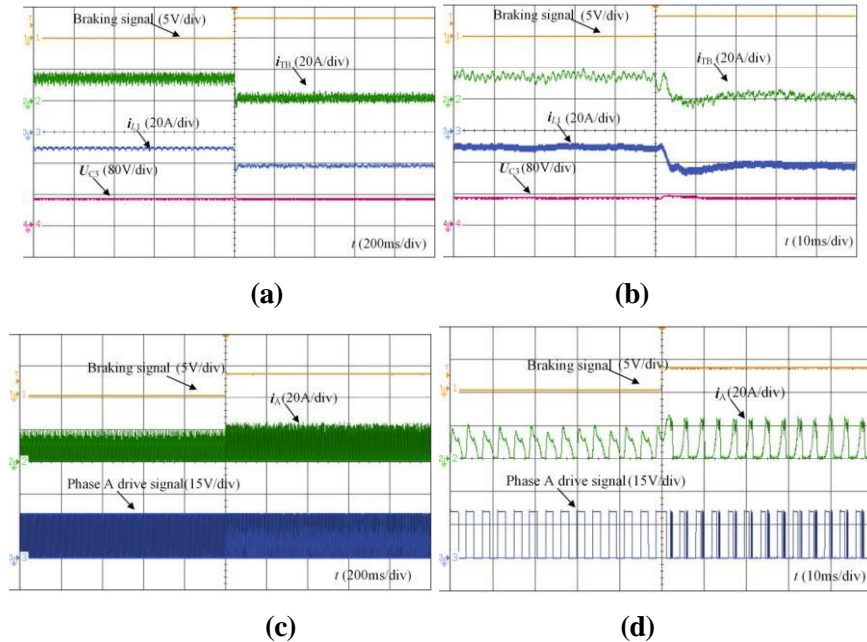


Figure.16 Switching process from motoring to braking operation. (a) i_{TB} , i_{L1} , U_{C3} . (b) Enlarged view of i_{TB} , i_{L1} , U_{C3} . (c) i_A , phase A drive signal. (d) Enlarged view of i_A , phase A drive signal.

4. Conclusion

This study proposes an optimised design for SRM drive converters used in PHEVs. This topology allows the PHEV to charge and drive simultaneously without relying on any additional power electronics components. Key contributions of the research include a proposal for an integrated power converter architecture that uses less circuit components including power semiconductor modules, inductors, and capacitors compared to the standard electrified powertrain for PHEVs. Adding only three relays allows for a wide range of driving modes and flexible charging options. The drive mode employs one of four operating modes—battery, engine, generator/traction battery hybrid, or regenerative braking—based on the load circumstances. The electric drive technology that is being suggested works better in high-speed service. A

three-channel interleaved boost PFC converter may be formed by the rectifier, SRM windings, and power converter during charging. This allows for increased charging power efficiency and minimised input current ripple. With the achievement of three charging modes—G2T, G2A, and T2A—the PHEV's charging versatility is enhanced. Capacitors C1 and C2, together with the rectifier, SRM windings, and power converter, serve several purposes in the suggested integrated converter's various modes of operation. Consequently, the electric drive system becomes more integrated, which in turn decreases both the cost and the volume. Also shown and validated via simulations are the associated control methods that integrate motor driving, adjustable power management, and battery-charging operations.

References

- [1] M. Ehsani, Y. Gao, and A. Emadi, *Modern Electric, Hybrid Electric and Fuel Cell Vehicles Fundamentals, Theory, and Design*. New York, NY, USA: CRC Press, 2010.
- [2] A. Khaligh and Z. Li, "Battery, ultracapacitor, fuel cell, and hybrid energy storage systems for electric, hybrid electric, fuel cell, and plug-in hybrid electric vehicles: State of the art," *IEEE Trans. Veh. Technol.*, vol. 59, no. 6, pp. 2806–2814, Jul. 2010.
- [3] M. Yilmaz and P. T. Krein, "Review of battery charger topologies, charging power levels, and infrastructure for plug-in electric and hybrid vehicles," *IEEE Trans. Power Electron.*, vol. 28, no. 5, pp. 2151–2169, May 2013.
- [4] P.-Y. Kong and G. K. Karagiannidis, "Charging schemes for plug-in hybrid electric vehicles in smart grid: A survey," *IEEE Access*, vol. 4, pp. 6846–6875, 2016.
- [5] C. M. Martinez, X. Hu, D. Cao, E. Velenis, B. Gao, and M. Wellers, "Energy management in plug-in hybrid electric vehicles: Recent progress and a connected vehicles perspective," *IEEE Trans. Veh. Technol.*, vol. 66, no. 6, pp. 4534–4549, Jun. 2017.
- [6] Z. Liu, D. Wang, H. Jia, N. Djilali, and W. Zhang, "Aggregation and bidirectional charging power control of plug-in hybrid electric vehicles: Generation system adequacy analysis," *IEEE Trans. Sustain. Energy*, vol. 6, no. 2, pp. 325–335, Apr. 2015.
- [7] H. Fathabadi, "Plug-in hybrid electric vehicles: Replacing internal combustion engine with clean and renewable energy based auxiliary power sources," *IEEE Trans. Power Electron.*, vol. 33, no. 11, pp. 9611–9618, Nov. 2018.
- [8] A. Emadi, Y. Joo Lee, and K. Rajashekar, "Power electronics and motor drives in electric, hybrid electric, and plug-in hybrid electric vehicles," *IEEE Trans. Ind. Electron.*, vol. 55, no. 6, pp. 2237–2245, Jun. 2008.
- [9] Z. Yang, F. Shang, I. P. Brown, and M. Krishnamurthy, "Comparative study of interior permanent magnet, induction, and switched reluctance motor drives for EV and HEV applications," *IEEE Trans. Transport. Electrification*, vol. 1, no. 3, pp. 245–254, Oct. 2015.
- [10] K. Kiyota, H. Sugimoto, and A. Chiba, "Comparing electric motors: An analysis using four standard driving schedules," *IEEE Ind. Appl. Mag.*, vol. 20, no. 4, pp. 12–20, Jul. 2014.
- [11] K. M. Rahman, B. Fahimi, G. Suresh, A. V. Rajarathnam, and M. Ehsani, "Advantages of switched reluctance motor application to EV and HEV: Design and control issues," *IEEE Trans. Ind. Appl.*, vol. 36, no. 1, pp. 111–121, Jan./Feb. 2000.
- [12] M. Takeno, A. Chiba, N. Hoshi, S. Ogasawara, M. Takemoto, and M. A. Rahman, "Test results and torque improvement of the 50-kW switched reluctance motor designed for hybrid electric vehicles," *IEEE Trans. Ind. Appl.*, vol. 48, no. 4, pp. 1327–1334, Jul. 2012.
- [13] A. Chiba, K. Kiyota, N. Hoshi, M. Takemoto, and S. Ogasawara, "Development of a Rare-Earth-Free SR motor with high torque density for hybrid vehicles," *IEEE Trans. Energy Convers.*, vol. 30, no. 1, pp. 175–182, Mar. 2015.